

Dr. Moneer Hameed Tolephih

The Micro-Slip Damper Stiffness Effect on the Steady-State Characteristics of Turbine Blade

Moneer H. Tolephih , Assistant Pro.

Abstract:

In this paper, a comprehensive study of friction damper stiffness effects on the response characteristics of a typical turbine blade executing steady-state motion, is explored. The damper is modeled as a one-bar microslip type assembled in the intermediate platform attachment of the blade leaving the other attachment of a shroud mass at the blade tip to be free. A discrete lumped mass approach, previously theorized in another paper, is employed to predict the response amplitudes as well as the slip length parameter at any state of the forced frequency including the resonance condition. The analysis covers a practical range of damper stiffness values adapted from relevant studies in this field. The present main outputs show that a magnificent rising of the response occurs with the increase in the stiffness, the characteristic behavior varies appreciably and the resonant amplitudes tend to increase linearly at high levels of damper stiffness, whereas the corresponding frequency and slip length show almost uniform trend. The results can serve very well for design and control purposes in the pre-manufacture stages of the given blade-damper system.

Keywords: Blade, stiffness .

1. Introduction:

The aspect of dry friction is occasionally found as a powerful tool to reduce high resonant stresses in industrial jet-engine blades[1], where serial assembled blades are attached together through platforms to maintain friction damping of the motion[2]. Generally, the steady-state motion characteristics depend widely upon the geometrical

and mechanical properties of the blade-damper system, the dry friction between mating surfaces of the damper play a role in describing the response behavior of the system[3]. The problem of friction modeling for reliable analysis of the process, becomes the major agency in relevant scopes of such subjects. The macroslip modeling type by Bazan et al [4], Ferri and Dowell[5], Muszynska and Jones[6], Wang et al [7], and the Microslip modeling by Meng et al [8,9,10], nonlinear vibration analysis for one dimensional dynamic microslip friction model and multi blade model by Cigeroglu et al [11,12] and Gabor[13], represent the professional attempts in this field. Each modeling approach bears lot of merits and some other demerits. Most advantages of the microslip friction modeling over the macro one, reflected in sophisticated representation of motion-dependency of the damping itself that can not take place in the macroslip class of friction. The excellent theoretical work, in this issue, may be found in references[8,13] where a proposition of one-bar friction modeling was displayed thoroughly, while the work of Meng et al [9] and Gabor[13] succeeds in creating a developed two-bar microslip model. The main difference between the two models is limited by the number of "slid" regions occupied in the friction plate of the damper which contains, for both models, one "stuck" region. However, the result governing equation of motion seems identical in the form regardless the type of friction bar modeling. In spite of that, there exists some difficulty in estimating the equivalent damper stiffness for the two model. The two-bar model show much lengthy manipulation of stiffness compared with the one-bar model. A group of input data should be prepared correctly for such analysis, these are consisting of all necessary parameters affecting the system response (the discrete lumped

masses and associated bending stiffness, the normal pressure variation in the damper mating surfaces, the Coulomb friction coefficient, the elastic constant, length and sectional area of the modeled bar). In his paper, the present author[14] investigated the effects of normal load parameters on the steady-state response comprehensively. Time comes now to extend the analysis to the friction damper effect regarding the elastic specification and geometry of the one-bar model (the physical length and sectional area). The author found that all these items can be gathered successfully in a single parameter referring to the damper longitudinal stiffness, without loss of originality, a matter which seems very important for quality control of the vibrated system and more essentially for mechanical design of the damping device itself.

2. Theoretical Analysis:

Keeping pace with the theoretical works of references[13], the present system of 2-degree of freedom, under consideration, is schematically shown in Fig.(1), with general notations used for analysis

purpose. The damper is attached to the lower platform of mass, m_1 , while a shroud mass, m_2 , is kept at the free end where an exciting harmonic force, P , is acting independently. The friction damper has an equivalent stiffness, k_{eq} , and damping constant, c_{eq} . Fig.(2) illustrates a possible normal pressure, q , acting on the mating surface of the damper plates whose Young modulus is denoted by E , length and sectional area by l and A respectively.

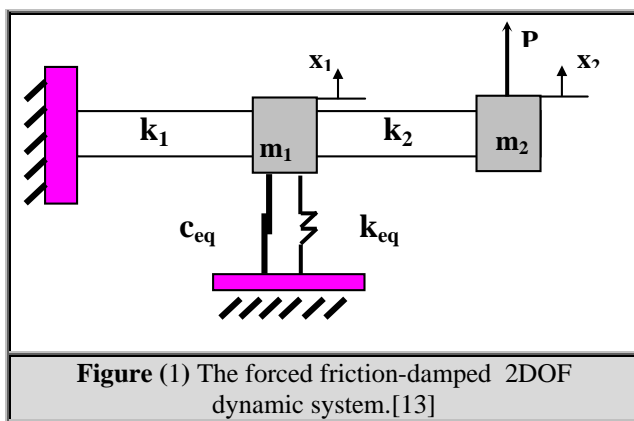


Figure (1) The forced friction-damped 2DOF dynamic system.[13]

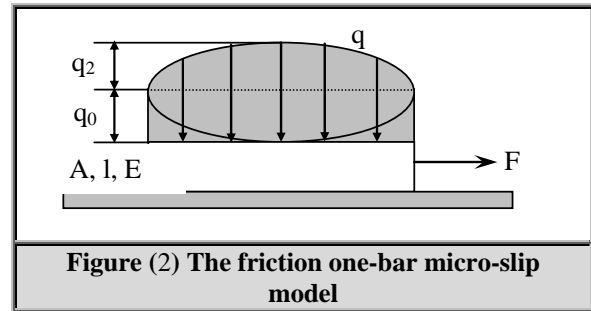


Figure (2) The friction one-bar micro-slip model

The plate, under friction action, is simulated as one-bar model, as shown in Fig.(3), with sliding part of length δ . The plate, in Figs.(2,3), is plotted at 900 rotation with that in Fig.(1). The piece-wise equation of motion, for the first and second mass of the given system, can be simplified in the following forms (see Ref.[15]):

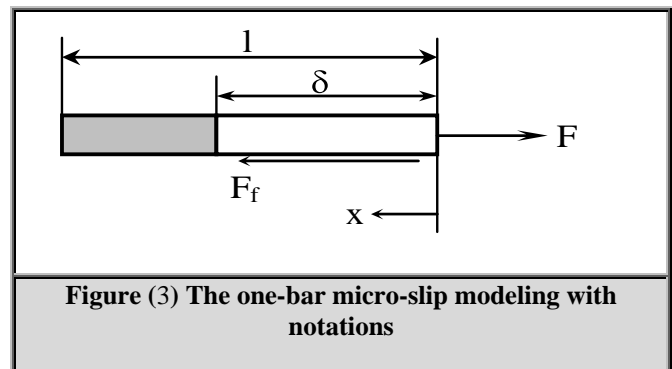


Figure (3) The one-bar micro-slip modeling with notations

$$\begin{aligned}
 m_1 \ddot{x}_1 + k_1 x_1 + k_2 (x_1 - x_2) + k_{eq} x_1 + c_{eq} \dot{x}_1 &= 0 \\
 m_2 \ddot{x}_2 + k_2 (x_2 - x_1) - P &= 0 \\
 P &= P_a e^{j\omega t} \\
 x_1 &= x_{1a} e^{j\omega t} \\
 x_2 &= x_{2a} e^{j\omega t}
 \end{aligned}$$

1

where x_1 and x_2 represent the displacement functions for the lower and upper attachments respectively, k_1 and k_2 the lumped bending stiffness respectively, P_a , x_{1a} and x_{2a} are the amplitudes of the exciting force and the piece-wise displacements respectively, while ω is the external frequency of the applied force and that j is the usual imaginary root and t is the elapsed time of excitation. To solve for the main response parameters x_{1a} , x_{2a} , then the substitution of the third of eq.(1), back into the first two equations, yields :

$$\begin{aligned}
 x_{1a} &= \frac{(P_a \cdot k_2)}{C_1 \cdot C_2 - k_2^2} \\
 x_{2a} &= \frac{(P_a + k_2 \cdot x_{1a})}{C_1} \\
 C_1 &= (k_2 - m_2 \cdot \omega^2) \\
 C_2 &= (k_1 + k_2 + k_{eq} + \omega c_{eq} \cdot j - m_1 \cdot \omega^2)
 \end{aligned}$$

Among all input data of (Pa, k1, k2, m1, m2 and ω) the indirect data keq and ceq, appearing in eq.(2) were usually estimated using Lazan[16] formula in the form of:

$$k_{eq} = \sqrt{\left(\frac{F_0}{u_0}\right)^2 - (c_{eq}\omega)^2}$$

where F0 and u0 are the amplitudes of the translated force and corresponding displacement, at the damper bar tip respectively (refer to Fig.(3)). In reference [14], a thorough derivation of both baranthes terms, in eq.(3), has been achieved successfully. The final expressions of these items may be summarized below:

$$\begin{aligned}
 \left(\frac{F_0}{u_0}\right) &= \frac{(EA/l)}{\Delta} \left[\frac{1 + \frac{2}{3} \frac{q_2}{q_0} (3\Delta - 2\Delta^2)}{\left[\frac{1}{2} + \frac{q_2}{q_0} \left(\frac{4\Delta}{3} - \Delta^2 \right) \right]} \right] \\
 c_{eq}\omega &= \frac{2(EA/l)}{3\pi\Delta} \left\{ \frac{\left[\frac{1 + \frac{q_2}{q_0} \left(4\Delta - \frac{14\Delta^2}{5} \right) \right]}{\left[\frac{1}{2} + \frac{q_2}{q_0} \left(\frac{4\Delta}{3} - \Delta^2 \right) \right]^2} + \frac{\left(\frac{q_2}{q_0} \right)^2 \left(\frac{8\Delta^4}{7} - 4\Delta^3 + \frac{16\Delta^2}{5} \right)}{\left[\frac{1}{2} + \frac{q_2}{q_0} \left(\frac{4\Delta}{3} - \Delta^2 \right) \right]^2} \right\} \\
 \Delta &= \frac{\delta}{1}
 \end{aligned}$$

Noting that the quantity (q2/q0) is simply the normal load ratio and Δ is the slip length ratio. The damper plate mechanical properties are evidently declared by the term (EA/l) appearing in above equation. It can be referred to one parameter entitled as the “damper longitudinal stiffness” whose effect stands as the main objective of the current work. In order to utilize eq.(4) the value of Δ must be pre-estimated. Gabor[13] has solved this problem by

equating u0 with x1a, as the matter should be recognized naturally. Reference [14] displays a “target function”, very useful to determine Δ upon usage of last idea, in the form of:

$$\begin{aligned}
 Q_0 &= \frac{\left(\frac{\Delta^2}{EA/l} \right) \left[\frac{1}{2} + \frac{Q_2}{Q_0} \left(\frac{4\Delta}{3} - \Delta^2 \right) \right]}{\frac{k_2}{(k_2 - m_2 \cdot \omega^2) \cdot (k_1 + k_2 + k_{eq} + \omega c_{eq} \cdot j - m_1 \cdot \omega^2) - k_2^2}} \\
 Q_0 &= \frac{mq_0 l}{P_a} \\
 Q_2 &= \frac{mq_2 l}{P_a}
 \end{aligned}$$

The introduced quantities Q0 and Q2 are just alternative forms of q0 and q2 respectively in non-dimensional fashion (with m denotes friction coefficient). The employment of eq.(5) needs further numerical method to assign the true value of Δ. An iteration procedure of “extended bi-secant” technique, familiarly found in related fields, may be very active to achieve the goal. At the end, the present computed results of x1a and x2a as varied with ω, would be conveniently altered to non-dimensional quantities of φ1, φ2 and Ω respectively in the form of:

$$\begin{aligned}
 \Omega &= \frac{\omega}{\omega_{e1}}, \quad \phi_1 = \frac{x_{1a}}{x_{1s}}, \quad \phi_2 = \frac{x_{2a}}{x_{2s}} \\
 \omega_{e1} &= \left[\frac{\left(\frac{k_1 + k_2}{m_1} + \frac{k_2}{m_2} \right)}{2} - \sqrt{\frac{\left(\frac{k_1 + k_2}{m_1} + \frac{k_2}{m_2} \right)^2}{4} - \frac{4k_1 k_2}{m_1 m_2}} \right]^{1/2} \\
 x_{1s} &= \frac{P_a}{k_1 + k_{eq}} \\
 x_{2s} &= \frac{P_a}{k_2} + x_{1s}
 \end{aligned}$$

where ωe1 denotes the first eign-frequency of the free-damped system, while x1s and x2s represent the “static” amplitudes respectively.

3. Numerical results and discussion:

First of all, a software program, built-up for present iteration procedure, is strictly run for fixed input data of: k1= k2=107N/m, m1= m1= m2=0.05kg, and

eight selected values of $Q_0=5.6, 16, 32, 80, 160, 320, 800$ and 8000 with $Q_2/Q_0=-0.5$. These are the actual constant parameters held well by [13,15]. In these references, the damper plate properties are kept constant with $EA=40000N$ and $l=0.2m$. In the present computation this is identical to $EA/l=200000$. Therefore, a choice of nine distinct values of (12500, 25000, 50000, 100000, 200000, 500000, 800000 and 860000), for this parameter, seem adequate to estimate the entire effect on the system. The plan is then devoted to spread the huge out printings of ϕ_1, ϕ_2 and Δ as related with Ω for given (EA/l) value, as well as the corresponding resonant parameters $\phi_{1res}, \phi_{2res}, \Delta_{res}$ and Ω_{res} as varied with the same damper stiffness. Figs.(4-15) and Tables(1-4) satisfy this condition briefly. In Figs.(4,5) the variation of ϕ_1 with Ω is plotted for fixed Q_2/Q_0 but for all the different values of (EA/l) . Fig.(4) takes the lowest set value of $Q_0=5.6$ whilst Fig.(5) takes the largest one $Q_0=8000$. As seen, the behavior is altered obviously. The peak points (resonant) go down with (EA/l) when Q_0 is small, whereas they go up for large Q_0 . The same trend can be noticed for ϕ_2 parameter as shown in Figs.(6,7) respectively and also for Δ parameter in Figs.(8,9) where at Ω approaches unity (from left or right), the peak Δ tends to equal one (i.e. the damper plate would totally slide). Tables(1-4) show a collection of resonant values of all the main parameters for a variety of settings of (AE/l) and Q_0 values keeping $Q_2/Q_0=-0.5$ as mentioned before. In each table, the data in the fifth row correspond to those recomputed from Gabor[13]. The figures, afterwards, relate to the resonant values as functions of the damper stiffness. The first two ones, in Figs.(10,11), show ϕ_{1res} variation for two setting values of Q_0 respectively. As shown, Fig.(10) illustrates a decreasing trend of ϕ_{1res} with (AE/l) for $Q_0=5.6$ to 80 , whereas Fig.(11) shows counter-wise linear trend for larger Q_0 value. The characteristic behavior, in this manner, seems new. The resonant curve decreases with Q_0 in Fig.(10), but it increases appreciably in Fig.(11). A similar style is observed in Figs.(12,13) for ϕ_{2res} parameter respectively with one exception that the counter-wise increase in ϕ_{2res} does not seem to be perfect linear. The last Figs.(14,15) show the variation of Δ_{res} and Ω_{res} with (EA/l) respectively for all the nine set values of Q_0 . In Fig.(14) the slip length ratio varies linearly with very slight increase, besides the curve itself goes down with Q_0 . A reversed behavior is noticed in Fig.(15) for Ω_{res} variation, where the ratio shows large increase, while it goes up as Q_0 increases further.

4. Conclusions:

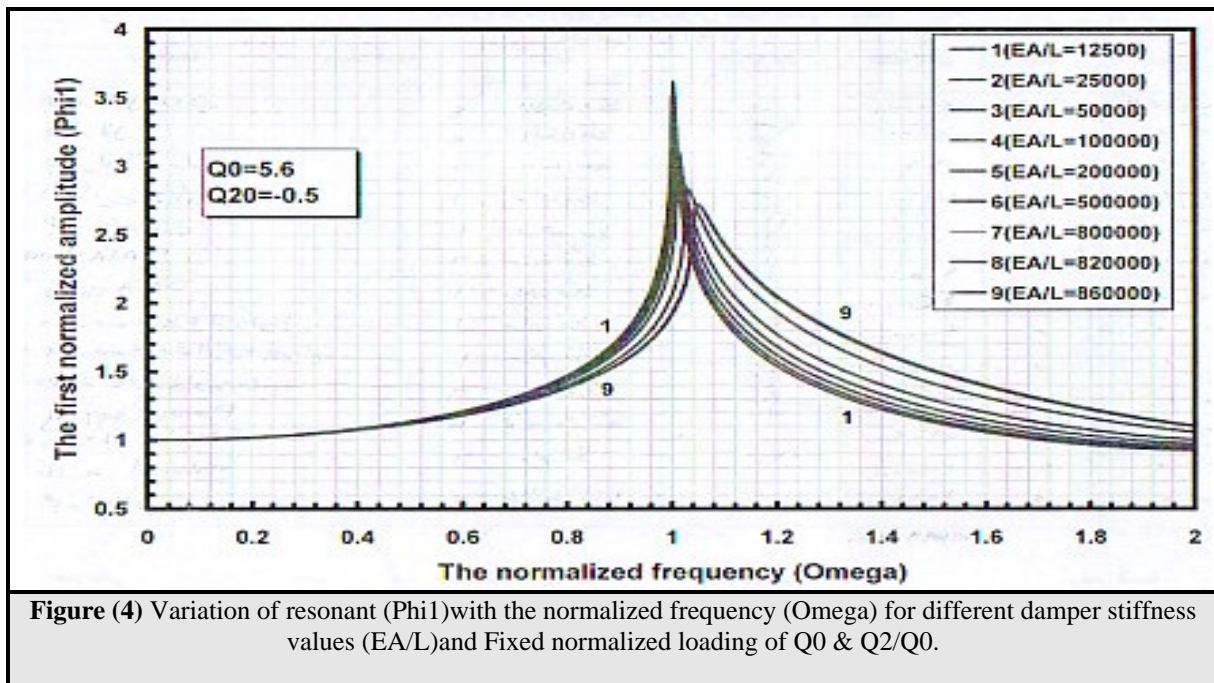
In brief, the pertinent remarks, listed below, represent the main conclusion drawn from present analysis and discussion:

- (a) The ϕ_1 and ϕ_2 response curves show special "shifting" with the increase in the exciting frequency as the damper stiffness increases. The artificial shift, for ϕ_1 , is in the down-right direction (i.e. the peaks decrease and move right with Ω), whereas for ϕ_2 the shift is in the up-right direction.
- (b) The Δ response curve rises with the damper stiffness and shows peak values near $\Omega=1$ when Q_0 is small. The stuck part length approaches maximum value at this situation. For large value of Q_0 the response curve goes up to the right with the increase in Ω .
- (c) The resonant displacements ϕ_{1res} and ϕ_{2res} show two different trends with (AE/l) . The first one concerns comparable small Q_0 value, where the curve goes down with both Q_0 and (AE/l) . The second one shows counter-wise manner absolutely with linear increase as (AE/l) increases.
- (d) The resonant curves, of slip length ratio Δ_{res} and frequency ratio Ω_{res} , give a humble linear rising with (AE/l) , but is strongly affected by Q_0 value. The characteristic curve of Δ_{res} goes down with the increase in Q_0 , whilst Ω_{res} curve shows a trend opposite to that comparably.

5. References:

1. Srinivasan A.V. and Cutts D.G., "Dry Friction Damping Mechanisms in Engine Blades", Trans. ASME, J. Engg. Power, 1983, Vol. 105, pp. 332-341.
2. Menq C.H., "A Review of Friction Damping of Turbine Blade Vibration", Int. J. Turbo & Jet Engines, 1990, Vol. 7, pp. 297-307.
3. Cameron T.M., "An Alternating Frequency/Time Domain Method for Calculating The Steady-State Response of Nonlinear Dynamic Systems", Trans. ASME, J. Appl. Mech., 1989, Vol. 56, pp. 149-154.
4. Bazan E., Beilak J. and Griffin J.H., "An Efficient Method for Predicting The Vibratory Response of Linear Structures With Friction Interfaces", Trans. ASME, J. Engg. Gas Turb. & Power, 1986, Vol. 108, pp. 633-640
5. Ferri A.A and Dowell E.H., "Frequency Domain Solutions To Multi-Degree-of-Freedom, Dry Friction Damped Systems", J. Sound & Vibr., 1988, Vol. 124, pp. 207-224.
6. Muszynska A. and Jones D.I., "On Tuned Bladed Disk Dynamics: Some Aspects of Friction Related Mistuning", J. Sound & Vibr., 1983, Vol. 86, pp. 107-128.
7. Wang J.H. and Sheih W.L., "The Influence of a Variable Function Coefficient On The Dynamic Behavior of a Blade With a Friction Damper", J. Sound & Vibr., 1991, Vol. 149, pp. 137-145.

8. Menq C.H., Griffin J.H. and Beilak J., "The Forced Response of Shrouded Fan Stages", Trans. ASME, J. Vibr. Acous. Stress & Reliab. In Design, 1986, Vol. 198, pp. 50-55.
9. Menq C.H., Bielak J. and Griffin J.H., "The influence of Microslip On Vibratory Response, Part I: A New Microslip Model", J. Sound & Vibr., 1986, Vol. 107, pp. 279-293.
10. Menq C.H., Bielak J. and Griffin J.H., "The influence of Microslip On Vibratory Response, Part II: A Comparison With Experimental Results", J. Sound & Vibr., 1986, Vol. 107, pp. 295-307.
11. Cigeroglu E., Lu W. and Menq C.H., "One-Dimensional Dynamic Microslip Friction Model", J. Sound and Vibr., 2006, Vol 292, pp881-898
12. Cigeroglu E, and Ozguven H., "Nonlinear Vibration Analysis of Bladed Disks with Dry Friction Dampers", J. Sound and Vibr., 2006, Vol 295, pp 1028-1043
13. Csaba G., Modelling Microslip Damping And Its Influence On Turbine Blade Vibrations, Dissertation No. 519, Linkoping Studies in Science and Technology, Linkoping University, Sweden, 1998.
14. Tolephih M.H., "The Normal Load Effect on Response Characteristics of Turbine Blades with One-Bar Microslip Friction Damper", sent for publication.
15. Timoshenko S.P, Young D.H. and Weaver W., Vibration Problems In Engineering, 4th Edition, 1974, John Wiley & Sons Inc., Canada.
16. Lazan B.J., Damping of Materials And Members in Structural Mechanics, 1968, Pergamon Press Inc., London.



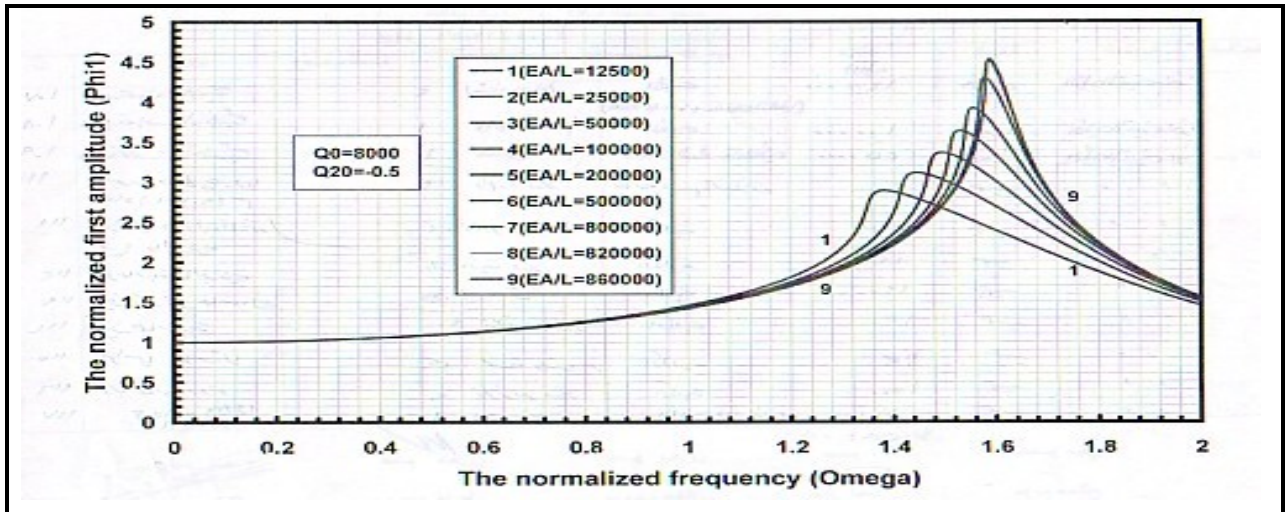


Figure (5) Variation of (Φ_1) with the normalized exciting frequency (Ω) for different damper stiffness values (EA/L) and fixed normalized loading of Q_0 & Q_2/Q_0 .

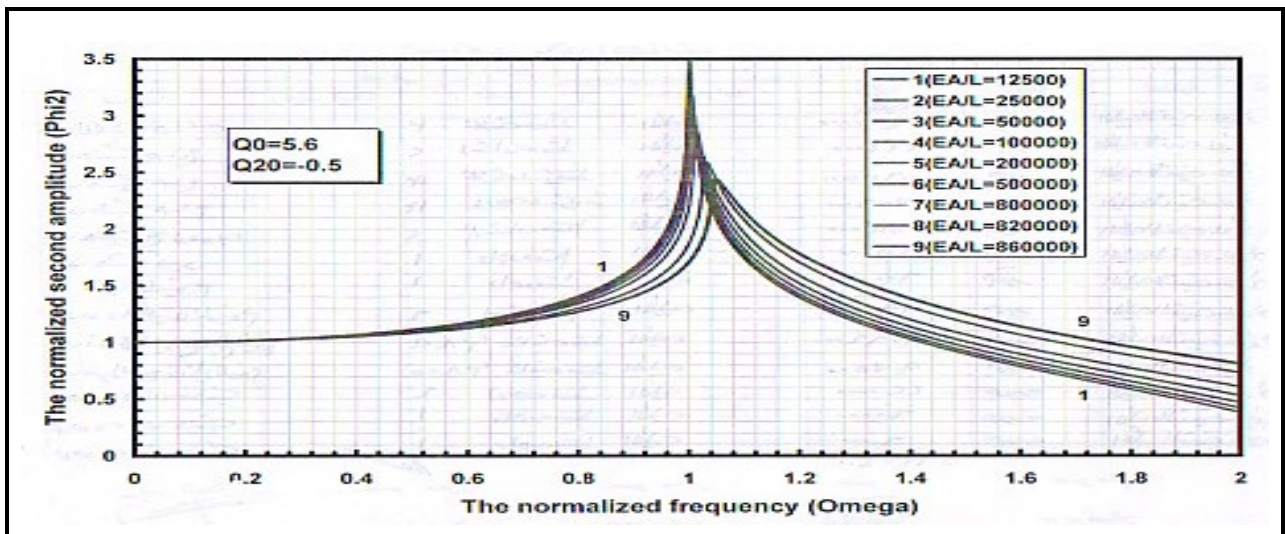


Fig.(6) Variation of resonant (Φ_2) with the normalized exciting frequency (Ω) for different damper stiffness values (EA/L) and fixed normalized loading of Q_0 & Q_2/Q_0 .

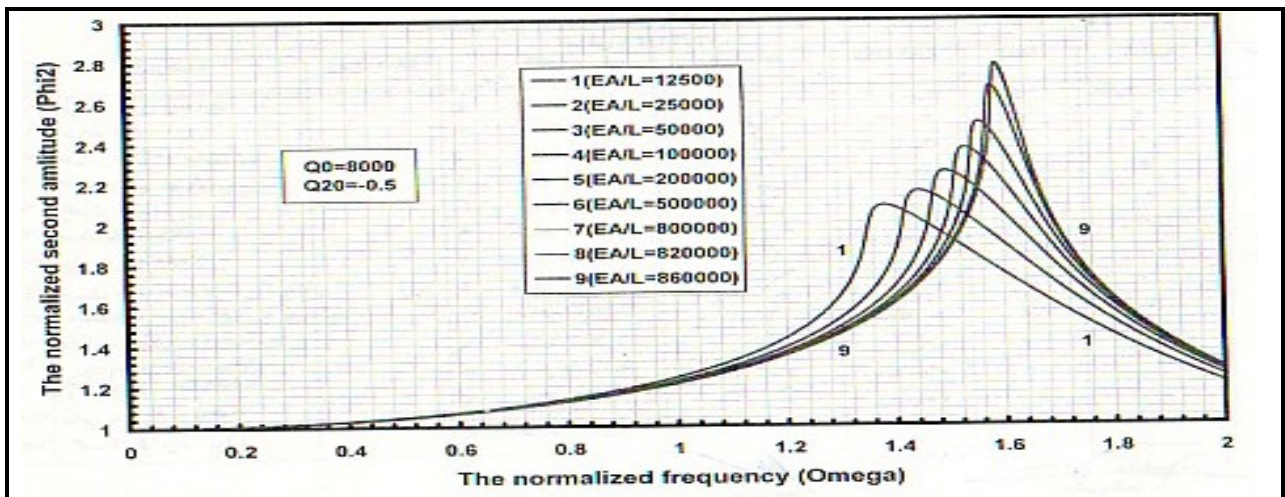


Figure (7) Variation of (Φ_2) with the normalized exciting frequency (Ω) for different damper stiffness values (EA/L) and fixed normalized loading of Q_0 & Q_2/Q_0 .

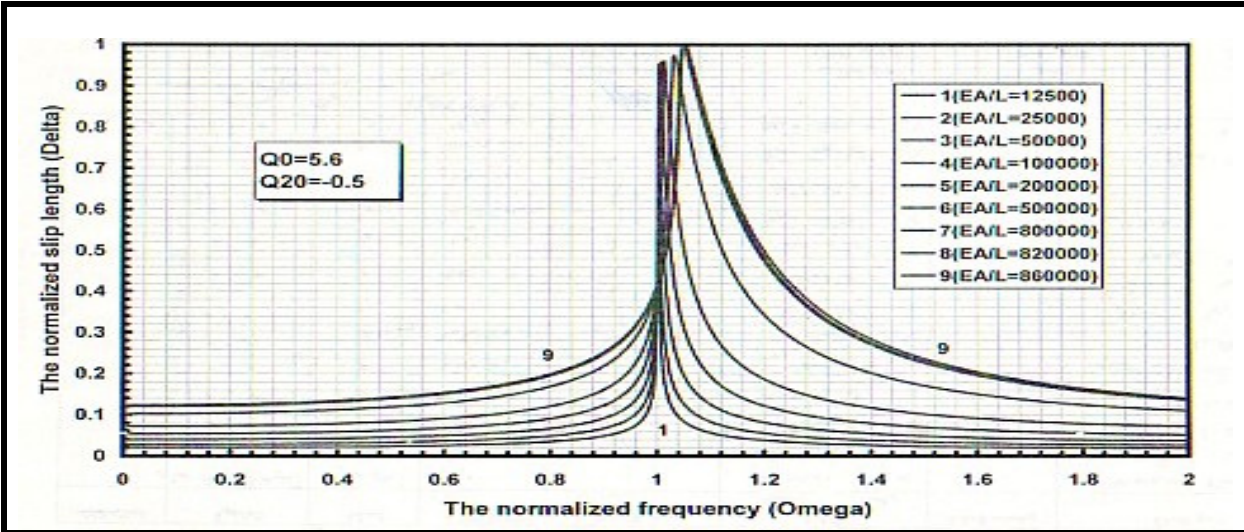


Figure (8) The resonant (Delta) as varied with normalized exciting frequency (Omega) for different damper stiffness values (EA/L) and fixed normalized loading Q_0 & Q_2/Q_0 .

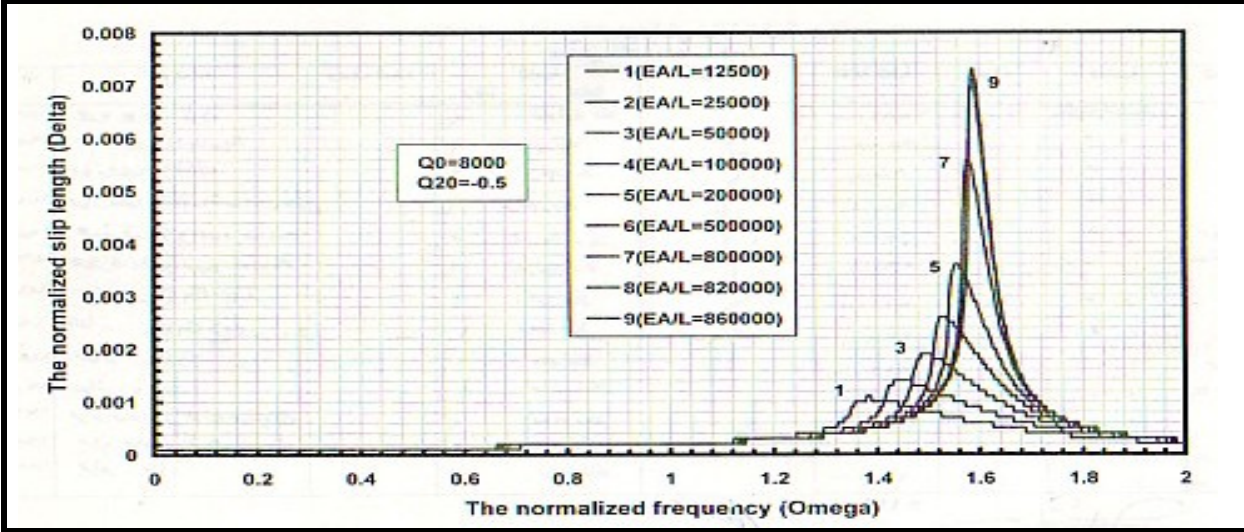


Figure.(9) The normalized (Delta) as varied with normalized exciting frequency (Omega) for different damper stiffness values (EA/L) and fixed normalized loading Q_0 & Q_2/Q_0 .

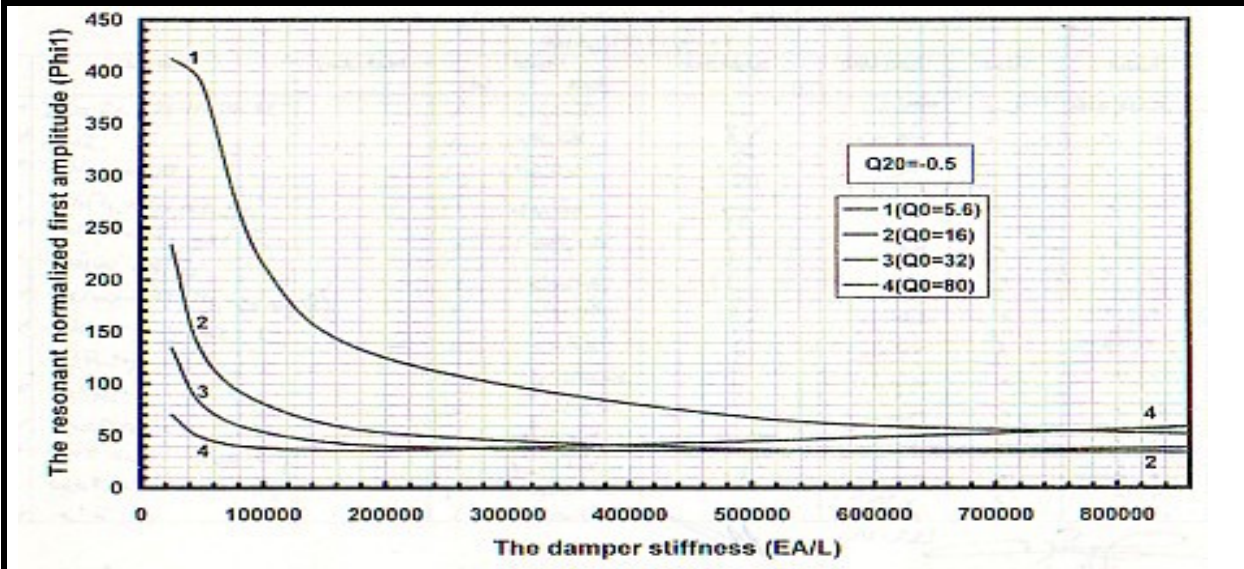


Figure (10) Variation of resonant (Phi1) with damper stiffness (EA/L) for fixed normalized load (Q_2/Q_0) and the first four values of the normalized load (Q_0).

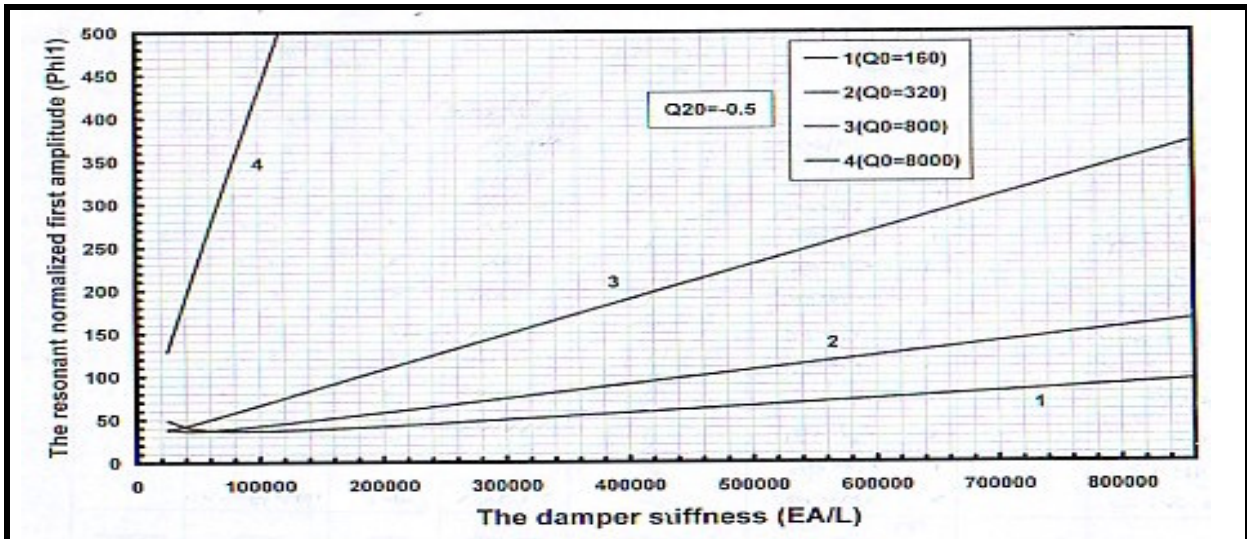


Figure (11) Variation of resonant (Φ_1) with damper stiffness (EA/L) for fixed normalized load (Q_2/Q_0) and the second four values of the normalized load (Q_0).

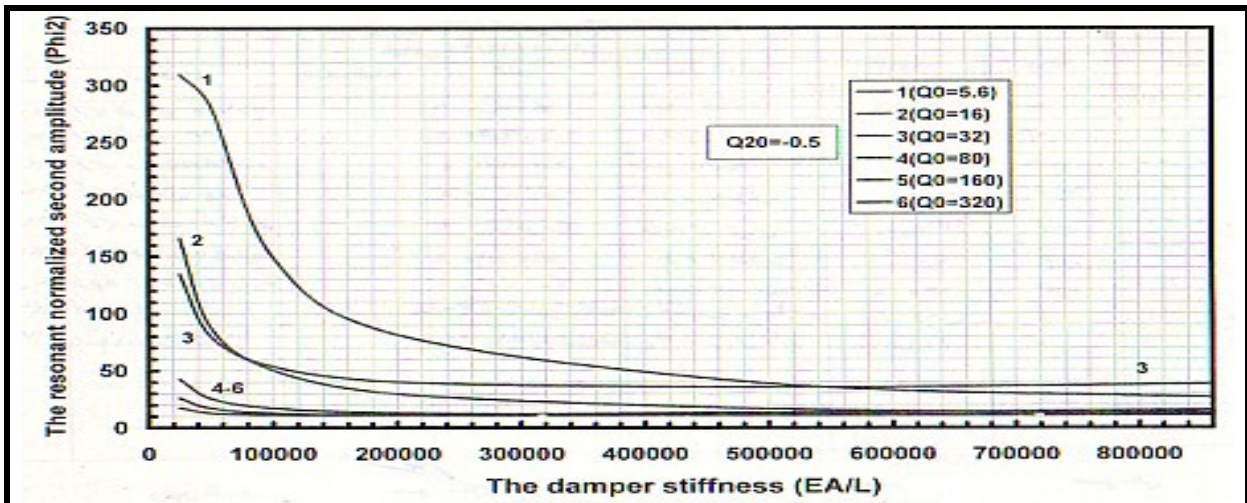


Figure (12) Variation of resonant (Φ_2) with damper stiffness (EA/L) for fixed normalized load (Q_2/Q_0) and the first six values of the normalized load (Q_0).

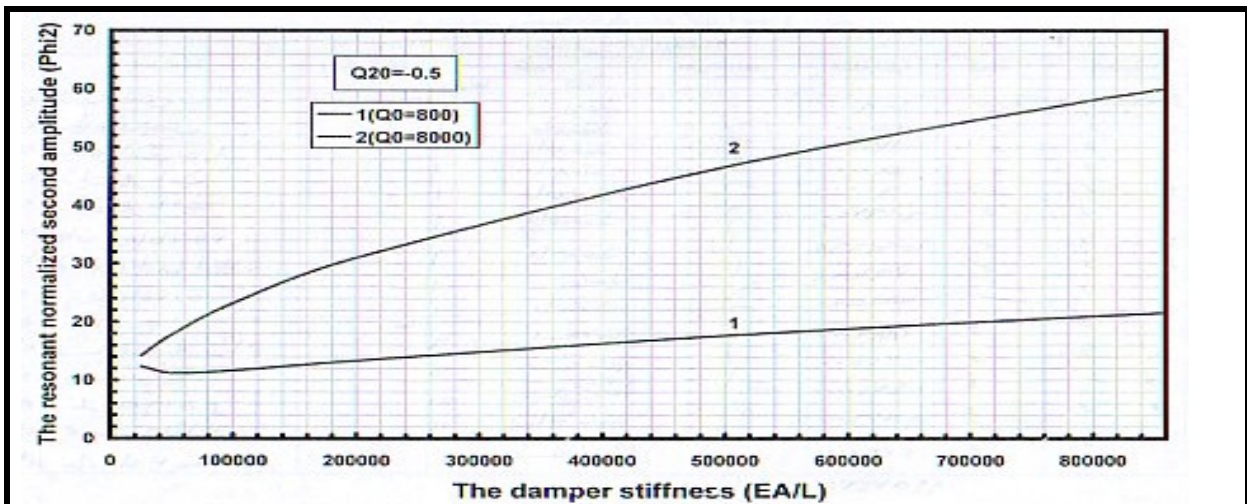


Figure (13) Variation of resonant (Φ_2) with damper stiffness (EA/L) for fixed normalized load (Q_2/Q_0) and the last two values of the normalized load (Q_0).

Table(1). The normalized amplitudes, slip lengths and frequencies at resonance for variety of damper stiffness values (EA/L) and two normal load coefficients ($Q_0=5.6, 16$).

Curve	EA/L	$Q_0=5.6$				$Q_0=16$			
		$\phi_{1,res}$	$\phi_{2,res}$	$\Delta_{a,res}$	Ω_{res}	$\phi_{1,res}$	$\phi_{2,res}$	$\Delta_{a,res}$	Ω_{res}
1	12500	358.3900	274.8890	0.4957	1.0033	430.7643	318.0713	0.2823	1.0033
2	25000	412.5412	309.3502	0.7500	1.0033	233.5297	165.9546	0.2829	1.0067
3	50000	388.3821	282.0630	0.9415	1.0033	131.1735	88.2626	0.2842	1.0133
4	100000	215.3262	149.4697	0.9462	1.0067	81.2281	50.5852	0.2945	1.0233
5(Gabor)	200000	125.1859	81.4756	0.9547	1.0133	53.1103	29.6315	0.3040	1.0433
6	500000	67.7086	38.7271	0.9736	1.0333	37.0060	16.6162	0.3322	1.0967
7	800000	53.5863	27.9348	0.9951	1.0500	34.3822	13.2966	0.3582	1.1367
8	820000	53.1490	27.5662	0.9973	1.0500	34.3294	13.1760	0.3599	1.1367
9	860000	51.9321	26.6350	0.9989	1.0533	34.2592	12.9176	0.3632	1.1433

Table(2). The normalized amplitudes, slip lengths and frequencies at resonance for variety of damper stiffness values (EA/L) and two normal load coefficients ($Q_0=32, 80$).

Curve	EA/L	$Q_0=32$				$Q_0=80$			
		$\phi_{1,res}$	$\phi_{2,res}$	$\Delta_{a,res}$	Ω_{res}	$\phi_{1,res}$	$\phi_{2,res}$	$\Delta_{a,res}$	Ω_{res}
1	12500	169.3906	169.3906	0.1304	1.0067	114.3412	75.2558	0.0502	1.0167
2	25000	134.4862	90.4921	0.1312	1.0133	70.3389	42.4752	0.0511	1.0300
3	50000	80.4874	50.1661	0.1330	1.0233	48.4170	25.8071	0.0532	1.0600
4	100000	53.7798	29.9858	0.1385	1.0467	38.3699	17.2400	0.0570	1.1033
5(Gabor)	200000	40.1684	19.1934	0.1467	1.0833	36.2025	12.9657	0.0637	1.1667
6	500000	35.4111	12.6673	0.1692	1.1633	45.0106	10.9932	0.0804	1.2733
7	800000	37.7586	11.1966	0.1891	1.2167	56.5110	11.0304	0.0940	1.3300
8	820000	37.9755	11.1414	0.1904	1.2200	57.2941	11.0466	0.0949	1.3333
9	860000	38.4143	11.0382	0.1928	1.2267	58.8478	11.0794	0.0965	1.3400

Table(3). The normalized amplitudes, slip lengths and frequencies at resonance for variety of damper stiffness values (EA/L) and two normal load coefficients ($Q_0=160, 320$).

Curve	EA/L	$Q_0=160$				$Q_0=320$			
		$\phi_{1,res}$	$\phi_{2,res}$	$\Delta_{a,res}$	Ω_{res}	$\phi_{1,res}$	$\phi_{2,res}$	$\Delta_{a,res}$	Ω_{res}
1	12500	70.1927	42.3300	0.0251	1.0333	48.7399	25.9845	0.0130	1.0600
2	25000	48.6410	25.9296	0.0262	1.0600	38.6195	17.3636	0.0139	1.1033
3	50000	38.5449	17.3260	0.0280	1.1033	36.6055	13.1073	0.0155	1.1700
4	100000	36.4692	13.0533	0.0313	1.1700	42.1323	11.3903	0.0182	1.2500
5(Gabor)	200000	41.9061	11.3204	0.0368	1.2500	57.8128	11.3214	0.0226	1.3333
6	500000	65.4657	11.4744	0.0497	1.3567	107.0689	13.2231	0.0322	1.4267
7	800000	89.7416	12.3961	0.0597	1.4067	155.5951	15.0678	0.0394	1.4633
8	820000	91.3779	12.4698	0.0603	1.4067	158.7989	15.1773	0.0398	1.4667
9	860000	94.5824	12.5890	0.0615	1.4133	165.2096	15.4034	0.0406	1.4700

Table(4). The normalized amplitudes, slip lengths and frequencies at resonance for variety of damper stiffness values (EA/L) and two normal load coefficients ($Q_0=800, 8000$).

Curve	EA/L	$Q_0=800$				$Q_0=8000$			
		$\phi_{1,res}$	$\phi_{2,res}$	$\Delta_{a,res}$	Ω_{res}	$\phi_{1,res}$	$\phi_{2,res}$	$\Delta_{a,res}$	Ω_{res}
1	12500	37.2405	15.6553	0.0057	1.1233	76.9926	12.0998	0.0011	1.3833
2	25000	37.5797	12.3708	0.0065	1.1933	128.8557	14.2304	0.0014	1.4467
3	50000	46.0021	11.2602	0.0077	1.2767	230.7795	17.8043	0.0019	1.4933
4	100000	66.3226	11.6577	0.0097	1.3567	430.6270	23.1904	0.0026	1.5300
5(Gabor)	200000	107.7988	13.3363	0.0127	1.4267	823.1804	30.9992	0.0036	1.5567
6	500000	229.4562	17.6633	0.0190	1.4933	1978.2296	46.6391	0.0056	1.5800
7	800000	348.5711	21.0105	0.0236	1.5200	3136.9676	58.1153	0.0070	1.5867
8	820000	356.4561	21.2149	0.0238	1.5200	3212.5258	58.7813	0.0071	1.5867
9	860000	372.2272	21.6083	0.0244	1.5233	3355.0038	60.0098	0.0073	1.5867

تأثير جساءة الانزلاق الماكروي على خصائص الحالة المستقرة للريش التوربينية

د. منير حميد طليح السعدي

استاذ مساعد

الكلية التقنية/ جامعة بغداد

الخلاصة:

تم في هذا البحث عرض دراسة موسعة لتأثير جساءة المخمد الاحتكاكي على الخصائص الاهتزازية لحركة الحالة المستقرة لنقطة اعتباطية في ريش التوربينات الصناعية. تم تمثيل المخمد رياضياً كنموذج أحادي القطعة ذي جزء منزلق احتكاكياً وآخر متلاصق سكونياً ومثبت في زعنفة كتلية في موقع وسطي من الريشة بينما ترك طرف الريشة الحر مربوطاً بزعنفة كتلية اعتباطية. اعتمدت طريقة الكتل المرصوصة المتقطعة كأسلوب رياضي لحل المنظومة المهتزة بقوة خارجية هارمونية التغير مع الزمن ومؤثرة في الطرف الحر من الريشة وأخذت في الاعتبار كل مواصفات التخميد المركب وحسابات الجساءة وثابت الإعاقة من وضعية (كابور-لازان) الرياضية والشغل المكافئ للدورة الاهتزازية الواحدة. غطى التحليل مدى مناسب من قيم صلابة المخمد العملية. إن أهم ما توصل إليه البحث هو إن هناك زيادة واضحة ومهمة في قيم استجابة المنظومة الرنينية مع زيادة الجساءة وتغير في شكل التصرف الميكانيكي السابق (عند ثبات الصلابة)، كما إن هذا التغير يكاد يصبح خطياً عند قيم عالية نسبياً للجساءة على عكس تلك التي تحدث لنسب طول منطقة الانزلاق حيث تضرع منحى للقيمة ثابت المقدار تقريباً. تشكل هذه النتائج بيانات مساعدة لأغراض السيطرة النوعية والتصميم الميكانيكي المسبق لصفحة التخميد الاحتكاكي.

This document was created with Win2PDF available at <http://www.daneprairie.com>.
The unregistered version of Win2PDF is for evaluation or non-commercial use only.